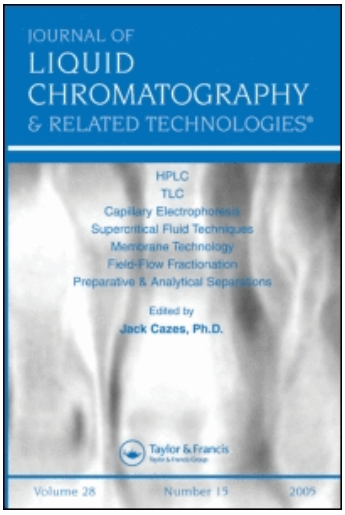

Journal of Liquid Chromatography & Related Technologies
Publication details, including instructions for authors and subscription information:
http://www.informaworld.com/smpp/title~content=t713597273

Chemometric Characterization of Chromatographic Retention Parameters of Mesoionic 1,3,4-Thiadiazolium-3-Aminides by Molecular Interaction Fields

Maria Luiza C. Montanari[a]; Anderson C. Gaudio[b]; Andrei Leitão[c]; Tânia M. G. de Almeida[c]; Carlos A. Montanari[d]
[a] Departamento de Química, Universidade Federal de São Carlos, São Carlos, SP, Brazil [b] Departamento de Física, Universidade Federal do Espírito Santo, Vitória, ES, Brazil [c] Núcleo de Estudos em Química Medicinal-NEQUIM, Universidade Federal de Minas Gerais, Belo Horizonte, MG, Brazil [d] Departamento de Química e Física Molecular, Instituto de Química de São Carlos, Universidade de São Paulo, São Carlos, SP, Brazil

To cite this Article Montanari, Maria Luiza C. , Gaudio, Anderson C. , Leitão, Andrei , de Almeida, Tânia M. G. and Montanari, Carlos A.(2006) 'Chemometric Characterization of Chromatographic Retention Parameters of Mesoionic 1,3,4-Thiadiazolium-3-Aminides by Molecular Interaction Fields', Journal of Liquid Chromatography & Related Technologies, 29: 3, 307 — 327
To link to this Article: DOI: 10.1080/10826070500451830
URL: http://dx.doi.org/10.1080/10826070500451830

Journal of Liquid Chromatography & Related Technologies®, 29: 307–327, 2006

ISSN 1082-6076 print/1520-572X online
DOI: 10.1080/10826070500451830

Chemometric Characterization of Chromatographic Retention Parameters of Mesoionic 1,3,4-Thiadiazolium-3-Aminides by Molecular Interaction Fields

Maria Luiza C. Montanari
Departamento de Química, Universidade Federal de São Carlos, São Carlos-SP, Brazil

Anderson C. Gaudio
Departamento de Física, Universidade Federal do Espírito Santo, Vitória, ES, Brazil

Andrei Leitão and Tânia M. G. de Almeida
Núcleo de Estudos em Química Medicinal-NEQUIM, Universidade Federal de Minas Gerais, Belo Horizonte, MG, Brazil

Carlos A. Montanari
Departamento de Química e Física Molecular, Instituto de Química de São Carlos, Universidade de São Paulo, São Carlos, SP, Brazil

Abstract: Mesoionic 1,3,4-thiadiazolium-3-aminides are described according to their properties of chromatographic partitioning. Log P_{app}^{RPLC} values obtained from C_{18} and in-house poly(methyloctylsiloxane) chromatographic columns correlated well with log P heteroatom contribution to overall lipophilicity. The pivotal role of partitioning from mobile to stationary phases is unraveled with GRID Molecular Interaction Fields, MIF. The descriptors extracted by the program VolSurf, resulted in partitioning being dependent on the hydrophilic-lipophilic balance. Volume-related terms and

Address correspondence to Carlos A. Montanari, Departamento de Química e Física Molecular, Instituto de Química de São Carlos, Universidade de São Paulo, PO Box 780, Av. Trabalhador Sancarlense, 400, 13560-970 São Carlos, SP, Brazil. E-mail: montana@iqsc.usp.br

electrostatics of the heterocyclic ring are of major importance in the retention mechanism.

Keywords: Chromatographic partitioning, RPLC, GRID/VolSurf, QSRR, Hydrophobic/hydrophilic balance, Heteroaromatic betaines

INTRODUCTION

Lipophilicity is an important physico-chemical parameter to be considered in drug design because drugs have to penetrate tissue fluids across tissue barriers. Lipophilicity can be either calculated or obtained experimentally.[1–4] A myriad of computer programs to calculate partition coefficients for neutral compounds in the system octanol/water can be found so far.[5–7] Nonetheless, for charged and betaine-like structures this is not a trivial task. Lipophilicity calculations rely on physico-chemical properties of compounds such as steric bulk, H-bonding, and electrostatics.[8–12] Adding up log *P* values in advance to compound synthesis is of special interest in quantitative structure activity relationship (QSAR) studies.[1,6,13] The H-bonding contribution to partitioning is the most difficult of all intermolecular forces encoded in lipophilicity to be calculated when predicting log *P* for heterocyclic compounds.[14,15] Therefore, the question that arises is related to the extent of a variable balance of hydrophobic and electrostatics forces that are involved in the partitioning of betaine-like structures,[16] such as the study mesoionic compounds, Figure 1.

Mesoionic compounds are dipolar five-membered heterocyclic compounds in which both the negative and the positive charges are delocalized throughout endo- and exo-cyclic atoms. A very covalent structure cannot be written, and these molecules cannot be represented without formal charges. Mesoionic 1,3,4-thiadiazolium-3-aminides have a stable five-membered ring and exhibit, among others,[17–22] biological activities of interest in medicinal chemistry.[20,23,24] As can be seen in Figure 1, the betaine-like structure (1) has a positive charge associated with the C5-N4-N3 (endo) moiety, which is counterbalanced by a negative charge at the N3-C2-N (exo) moiety.[25–27] Its hydrochloride might be represented by structure (2), which is in agreement with spectrometric studies and X-ray

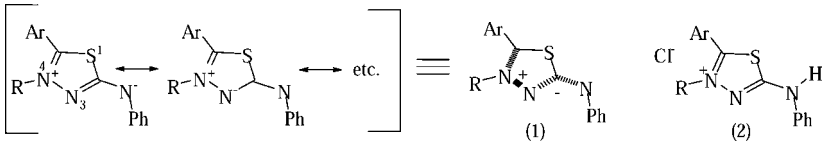

Figure 1. Structure representation of study of mesoionic 1,3,4-thyadiazolium-3-aminides.

crystallographic data.[28,29] Moreover, the description of molecular interactions by screening charge densities gives an integrated understanding of electrostatics and lipophilicity, which often are considered separate physical entities in molecular field analysis tools.

When performing quantitative structure property relationship, QSPR, studies, the lipophilicity constant, π, is of great importance, too. It can be obtained from either tables or computer calculations. Nevertheless, to the best of our knowledge this is not so easy for compounds such as those shown in Figure 1.

Nearly all-molecular retention behavior is exerted by an interaction with a stationary phase. This involves a specific molecular interaction between the solute and the phase. To date, little information has been accumulated about the relationships between structure and chromatographic retention of such compounds.[30,31] In order to circumvent this, the quantitative structure-property relationship, QSPR, analysis has proven to be of interest in the understanding of molecular properties and their structures.[32,33,34]

Chromatographic retention factor, k,[35–39] provides a straightforward way of measuring the partition coefficient at a fixed pH (log P_{app}^{RPLC}) of a molecule eluting in many mobile and stationary phases. It can be used as a qualitative measure of entropy of solvent.[40–43] To investigate these properties through QSPR studies, we have synthesized eight mesoionic compounds[44] and determined their partitioning, log P_{app}^{RPLC}, using reversed phase high performance liquid chromatography, RPLC.[35] Log k_w, the extrapolated log k for 0% of modifier content, was calculated and used as chromatographic partitioning coefficient. The aim of this paper is to show that log P can be calculated from atom-based procedures and correlated with log P values obtained from RPLC measurements. It is also aimed at the identification of the physico-chemical parameters needed to depict the partitioning behavior through their 3D molecular interaction fields, MIF. The main goal is to find the reasons chiefly encoded in the properties of mesoionic molecules responsible for the chromatographic partitioning process to take place.

EXPERIMENTAL

The mesoionic compounds screened against the two columns depicted in this paper were synthesized according to the previously published procedure.[44]

The RP-HPLC experiments were recorded on a Schimadzu instrument equipped with two bombs LC-10AD, UV detector SPD-6AV, and LC-R6A. The stationary phase was a C_{18} ODS-Shin-Pack column (18.0 × 6.0 mm). The mobile phase was a buffer of 5.10^{-3} M of phosphoric and glacial acetic acids at pH 4.6 and methanol as modifier agent. An in-house HPLC column made of poly(methyloctylsiloxane), PMOS 50%,[45] was also used to evaluate its capability of disclosing log P for such compounds.

The X-ray crystallographic data for compound 7, were collected from CCDC and used as starting geometry for the simulation of other mesoionic 3D structures.[29] The molecular modeling maneuvers were carried out via Sybyl 6.5.3 software.[46] Log *P* calculations from the atom based procedure avoid correction rules, but define a number of atom types where lipophilicity is quantified by the summation of atom-type value. The 3D TSAR software[47] was chosen as a tool for calculating the partition coefficient ($\mathrm{Clog\,P_{TSAR}}$) for the study of all mesoionic compounds: Table 1 shows the results.

The understanding of the chromatographic retention mechanisms played by these compounds was accomplished by the use of the GRID/VolSurf procedure.[48,49] This powerful computer automated approach has been used to correlate 3D MIF with physicochemical and pharmacokinetic properties.[23,50,51] First, it generates MIF by using the GRID program,[52–55] then it treats the fields accordingly by producing descriptors that encode the information content from the chosen water and hydrophobic probes. VolSurf has the advantage of producing descriptors (Table 2) using the 3D information embedded in any map. VolSurf is also alignment independent and conformation insensitive. The VolSurf transformation is fast and its results are easy to interpret. The descriptors have a clear chemical meaning and are lattice-independent. Work reported herein demonstrates the usefulness of the method in describing the partition coefficients obtained from an HPLC technique. There is a chemical interpretation of VolSurf descriptors, which is outlined herein. However, readers are referred to the specialized literature on this subject for a more detailed description.[56] The interaction of molecules with biological membranes is mediated by surface properties. These properties are determined from the size, shape, electrostatics, and hydrophobicity obtained from calculations. Size and shape descriptors encode molecular volume, surface, globularity, and the ratio volume/surface, and they are explained in Table 2. Descriptors of hydrophilic regions include a molecular envelope that is accessible to, and attracts water molecules, and capacity factors that are represented by the hydrophilic surface per total molecular surface unit. Capacity factors are proportional to the concentration of exposed polar groups compared to the total surface area, and are often relevant in membrane partitioning in which solvation–desolvation processes are of critical importance. The interaction energy (integy) moments express, like dipole moments, the unbalance between the center of mass of a molecule and the barycenter of its hydrophilic regions.[57] The integy moment is calculated for both hydrophilic and hydrophobic regions. For the first, they are vectors pointing from the center of mass to the center of the hydrophilic regions, whereas for the latter, they measure the unbalance between the center of mass of a molecule and the barycenter of the hydrophobic regions. The high integy moments depicted in this study (see Figure 6) suggest a concentration of hydrated region in one part of the molecule. The hydrophilic–lipophilic balance is the ratio between the hydrophilic and the hydrophobic regions. The descriptors of

Table 1. Chromatographic partitioning coefficients, log K_w, obtained from ODS and PMOS columns, and their related values

No.	Compounds[a]	log P (ODS)[b]	log k_w (ODS)	π_{kw}	log P (PMOS)[c]	log k_w (PMOS)	π_{kw}	Clog P_{TSAR}[d]
1	$Ar_1 = C_6H_5$ R = Me	1.74	1.93	0.00	1.65	1.83	0.00	4.50
2	$Ar_1 = p$-Me-C_6H_4 R = Me	2.29	2.44	0.51	2.18	2.28	0.45	4.97
3	$Ar_1 = p$-MeO-C_6H_4 R = Me	2.02	2.19	0.26	1.94	2.07	0.24	4.25
4	$Ar_1 = p$-$_2$ON-C_6H_4 R = Me	1.66	1.85	−0.07	1.58	1.76	−0.07	4.45
5	Ar_1 = R = Ph	2.86	2.96	0.00	2.78	2.79	0.00	6.41
6	$Ar_1 = p$-Me-C_6H_4 R = Ph	3.64	3.68	0.72	3.34	3.28	0.49	6.88
7	$Ar_1 = p$-MeO-C_6H_4 R = Ph	3.11	3.19	0.23	2.95	2.94	0.15	6.16
8	$Ar_1 = p$-$_2$ON-C_6H_4 R = Ph	3.10	3.18	0.22	2.86	2.86	0.07	6.37

[a]All compounds have been prepared and described elsewhere. See reference [44] for experimental details.

[b]Log P values obtained from Collander type equation: $\log k_w = 0.92(\pm 0.13)\log P_{oct} + 0.32(\pm 0.30)$, (n = 9, $r^2 = 0.974$, $s = 0.119$, F = 263.0, $Q^2 = 0.960$). See reference [30] for details.

[c]Log P values obtained from Collander type equation: $\log k_w = 0.86(\pm 0.18)\log P_{oct} + 0.41(\pm 0.38)$, (n = 9, $r^2 = 0.949$, $s = 0.157$, F = 130.9, $Q^2 = 0.904$). This equation was obtained in accordance with reference 30.

[d]Log P values calculated via atom based from 3D TSAR software [47].

Table 2. The VolSurf descriptors[a]

1. V Volume: total volume (computed at 0.25 kcal mol^{-1})	2. S Surface: total surface (computed at 0.25 kcal mol^{-1})
3. R Rugosity: total volume/total surface	4. G Globularity: surface of the compound divided by the surface of a sphere with the same volume
5–12. W1-W8 Volume of interaction with the H2O probe at −0.2, −0.5, −1.0, −2. 0, −3.0, −4.0, −5.0, and −6.0 kcal mol^{-1} levels	13–20. IW1-IW8 Integy moment: proportional to the distance between the barycentre of the surface and the volume of interactions with the H2O probe at the above energy levels
21–28. CW1-CW8 Capacity factor: volume of interaction with the H2O probe divided by the surface	29–31. Min1-Min3 Energy minima: the first three energy minima interactions
32–34. D12, D13, D23 Distance: the distances between the energy minima	35–42. D1-D8 Volume of interaction with the DRY probe at −0.2, −0.4, −0.6, −0.8, −1.0, −1.2, −1.4, and −1.6 kcal mol^{-1} levels
43–50. ID1-ID8 Integy moment: proportional to the distance between the barycentre of the surface and the volume of interactions with the DRY probe at the different energy levels	51–52. HL1, HL2 Balances of the hydrophilic-hydrophobic interactions, measured at −4 and −0.8 kcal mol^{-1}
53. A Amphiphilic moment	54. CP Critical packing
55. POL Molecular polarizability	56. MW Molecular weight

[a]Depicted VolSurf descriptors refer to maps of the druglike chemical space for relevant pharmacokinetic properties.

hydrophobic regions are molecular envelopes generating attractive hydrophobic interactions. All calculations were performed on a R10000 O2 Silicon Graphics workstation. Polarizability values were used to calculate fields for atom type N═.

RESULTS AND DISCUSSION

Transport from Mobile Phase to Stationary Phase

Partitioning is a term that may be coined to express the solute ratio between stationary and mobile phases. Its coefficient can be expressed as log k. Out of many different ways of obtaining partition coefficient values for compounds with biological interest, our research interest is focused on chromatographic partition coefficients.[30,58–60]

Partitioning in RPLC deals with the escape of the molecule from mobile phase to the surface of the stationary phase. The hydrocarbon coating forms a "molecular fur" where lipophilic molecules can interact. The retention factor of the solute, log k, cannot be obtained for most molecules solely in neat water. Thus, a cosolvent (35%–75% methanol content in this study) is added. At fixed pH, k is an apparent chromatographic partition coefficient. The extrapolation to zero content of the cosolvent yields k_w, which is so expressed in Table 1. This extrapolated k_w for neat water, can then be used as chromatographic partition coefficient, and thus, be related to transport from buffer to more structured media. Furthermore, transport can be dependent on molecular properties of 3D structures, lipophilicity, H-bonding, and the ratio between polar and apolar molecular surfaces.

Table 1 shows the chromatographic partitioning data, obtained from RPLC measurements, log k_w, and calculated log P values for two stationary phases: octadesyl silica, ODS, and the in-house poly(methyloctylsiloxane), PMOS.[45] Calculated log P, with the atom contribution via TSAR software, can also be found in Table 1. Equations (1) and (2) show the linear correlations for log k_w, the chromatographic partition coefficient in "neat water", and TSAR calculated log P values (Clog P_{TSAR}). Equations (3) and (4) show the linear relationships between Clog P_{TSAR} and log P obtained from C_{18} and PMOS columns, log P_{ODS}, and log P_{PMOS}, respectively.

$$\log k_{w(ODS)} = 0.60\ (\pm 0.06)\ \text{Clog}\ P_{TSAR} - 0.65\ (\pm 0.39)$$
$$(n = 8;\ r^2 = 0.920;\ s = 0.204;\ F = 69.33;\ Q^2 = 0.876) \quad (1)$$

$$\log k_{w(PMOS)} = 0.51\ (\pm 0.06)\ \text{Clog}\ P_{TSAR} - 0.88\ (\pm 0.38)$$
$$(n = 8;\ r^2 = 0.927;\ s = 0.166;\ F = 75.81;\ Q^2 = 0.876) \quad (2)$$

$$\log P_{ODS} = 0.65\ (\pm 0.07)\ \text{Clog}\ P_{TSAR} - 1.01\ (\pm 0.42)$$
$$(n = 8;\ r^2 = 0.921;\ s = 0.218;\ F = 69.48;\ Q^2 = 0.876) \quad (3)$$

$$\log P_{PMOS} = 0.60\ (\pm 0.07)\ \text{Clog}\ P_{TSAR} - 0.88\ (\pm 0.44)$$
$$(n = 8;\ r^2 = 0.927;\ s = 0.193;\ F = 75.89;\ Q^2 = 0.876) \quad (4)$$

The above equations have almost the same slope magnitudes (ca. 0.60). Since the same set of compounds was eluted against the two columns, a Collander type equation was derived (Equations (5) and (6)). The slopes are near 1 and intercept near zero, which represents the evidence that the two columns behave similarly according to their partitioning environments. The same set of compounds is eluting against the two different stationary phases

on the basis of the similar topographic relations and hydrophobic binding interactions.

$$\log P_{\mathrm{PMOS}} = 0.92\ (\pm 0.07)\ \log P_{\mathrm{ODS}} + 0.07\ (\pm 0.02)$$
$$(\mathrm{n} = 8;\ r^2 = 0.997;\ s = 0.051;\ \mathrm{F} = 1159.90;\ Q^2 = 0.991) \qquad (5)$$

$$\log k_{\mathrm{W(PMOS)}} = 0.84\ (\pm 0.06)\ \log k_{\mathrm{W(ODS)}} + 0.22\ (\pm 0.02)$$
$$(\mathrm{n} = 8;\ r^2 = 0.994;\ s = 0.044;\ \mathrm{F} = 1172.10;\ Q^2 = 0.991) \qquad (6)$$

Lipophilic Constant, π

The estimation of additive-constitutive behavior of log P,[6a] can be accomplished through the free-energy-related property of partitioning. It is calculated according to the equation: log $P = \mathrm{a}\ \log P_{\mathrm{H}} + \Sigma\pi_{\mathrm{xi}}$, where H represents the unsubstituted molecule and π is the lipophilic contribution of a substituent.

In order to examine whether the additivity holds true for the study of mesoionic compounds, we have calculated their chromatographic lipophilic constants, π_{HPLC}, Table 1. The $\pi_{\mathrm{RPLC\text{-}ODS}}$ for Me (π_{Me}) resembles the one substituted on phenyl rings, which is 0.56[6b] (our value 0.51) for mesoionic 2. The value rises to 0.72 for compound 6, the average value for π_{ortho} and π_{para} substituted phenyl rings. This accounts for the higher π contribution of the phenyl moiety as compared to Me's. In the same trend comes the $\pi_{\mathrm{NO_2}}$: -0.07, our calculated value for compound 4 against -0.28 for π_{benzol} and 0.22 for 8 against 0.22 of π_{para} substituted phenyl rings. Surely, this later value gives the expected π contribution of nitro groups as being of lipophilic character. The changing in this behavior according to substitution at N4-position of the mesoionic ring is remarkable. This seemingly straightforward result is in good agreement with VolSurf analysis of GRID Molecular Interaction Fields, MIF, (see below for explanation). Nevertheless, this does not hold true for compound 8. The methoxy 4-substituted phenyl ring has raised no real distinction among π values for study compounds, rather than being of lipophilic character as generally observed in π_{meta} phenyl moieties.

GRID/VolSurf Descriptors and Their Role in Log $k_{\mathrm{w}}^{\mathrm{RPLC}}$

Calculated molecular properties from 3D molecular structure fields can be of value in accounting for RPLC partitioning. The interaction energies between chemical probes and analytes yield valuable information on the nature of retention mechanisms. The GRID force field, which is one of the most widely used computational tools to map putative molecular surfaces, was applied to calculate 3D molecular interaction fields (MIF) for all mesoionic

study. These fields were converted automatically to simpler molecular descriptors through the VolSurf procedure. In this method, interaction fields with water and hydrophobic DRY probes were calculated all around the target molecules. The 3D MIF content was quantitatively evaluated through the implemented PLS tool. These descriptors are mostly supposed to be related to pharmacokinetic properties,[57,61] though they can be applied for any type of molecular interaction, including counterions, cofactors, receptor-ligand complexes, and chromatographic partitioning coefficients.

The calculated water and DRY MIF generated very similar results in all analyses. They are fully discussed in this paper for chromatographic partition coefficients, log k_w^{RPLC} obtained from the PMOS in-house column, notwithstanding the Table 3 shows all PLS results.

Figure 2 represents the PLS scores plot (PC2 *versus* PC1). PC1, which accounts for 29.3% of total variance (ca. 81% for the three first principal components), is able to discriminate both sets of mesoionic compounds, according to their Me or Ph N4-substitutions. Compounds (1–4) with lower values of log $k_{w(PMOS)}$ can be found at negative PC1 values, whereas compounds (5-8) with higher log $k_{w(PMOS)}$ are allocated at positive PC1 values. The relationship between log $k_{w(PMOS)}$ and calculated VolSurf descriptors analyzed by partial least-squares projection to latent structures is shown in Figure 3. The good fit for the two component model explains 93% of total variance with a predictive power of 69%.

Figure 4 shows the PLS loading plot for the two first PCs. The Y1 represents the chromatographic retention. The (+, +) quadrant has mostly size and shape descriptors, the (+, −) is a mixture of descriptors of hydrophilic and hydrophobic regions, the (−, −) is essentially of hydrophilic and (−, +) of hydrophobic regions. It can be deduced that size and shape descriptors (G, S, V) are positively correlated with chromatographic partitioning. The hydrophobic regions, D, amphiphilic moment (A), and critical packing factor (CP) are

Table 3. PLS models for all VolSurf analyses

Analyses	r^{2a}	Q^{2b}	Components	SDEC[c]	SDEP[d]
log $k_{w(ODS)}$	0.919	0.647	2	0.177	0.327
log $k_{w(PMOS)}$	0.929	0.687[e]	2	0.141	0.296
log $P_{(ODS)}$	0.921	0.651	2	0.191	0.402
log $P_{(PMOS)}$	0.929	0.687	2	0.249	0.345
log $P_{(TSAR)}$	0.975	0.848	2	0.158	0.387

[a]How well the PLS analysis fits the data.

[b]PLS analysis validation with leave-one-out accounting for prediction power of the model.

[c]Standard deviation of estimated calculation.

[d]Standard deviation of estimated prediction.

[e]Leave-two-out, $Q^2 = 0.658$, 4 random groups out, $Q^2 = 0.670$.

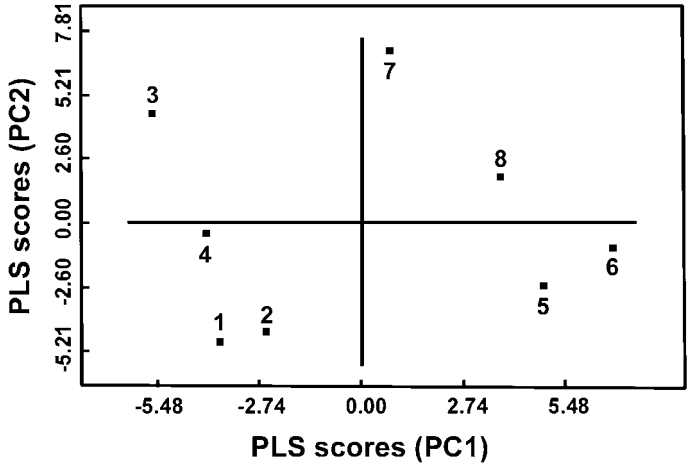

Figure 2. PLS score plot for PC2 versus PC1.

favorable for partitioning, too. On the other hand, interaction energy moments (Iw, ID) and capacity factors (Cw) are negatively correlated with partitioning.

In order to verify the importance of fitting and predicting power of the model, we have graphed r^2 and Q^2 against the number of components needed to describe the model. As can be seen from Figure 5, both parameters are fairly in agreement with the increase of the components number. This is very important due to the fact the prediction does not fall apart with an increasing number of components. Thus, the robustness of such a result is a guarantee the chromatographic partitioning is being well weighted in the PLS analysis according with the correct number of components.

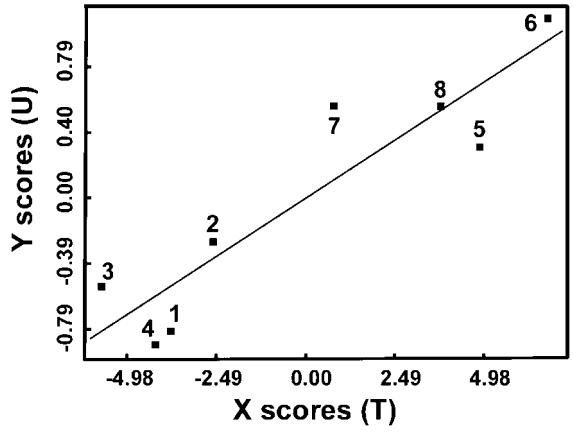

Figure 3. PLS plot of the correlation between the VolSurf descriptors (T1) and log $k_{w(PMOS)}$.

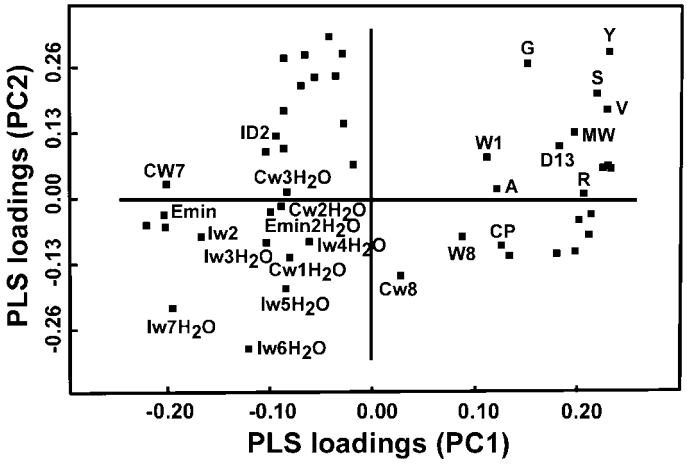

Figure 4. PLS loading plot (partial weights) of PC1 *versus* PC2 for the model of Figure 3. Y1 represents the dependent variable of partitioning.

PLS Coefficients

The interpretation of PLS coefficient plots is useful to understand the meaning of the descriptors shown in Figure 4. Figure 6 shows the corresponding coefficient plot for PC1. The vertical bars represent the contribution of a single descriptor: short ones are not important, whereas longer ones are important descriptors. The log k_w^{RPLC} values are positively correlated with the size and shape, namely the molecular volume, surface, the ratio volume/surface, and

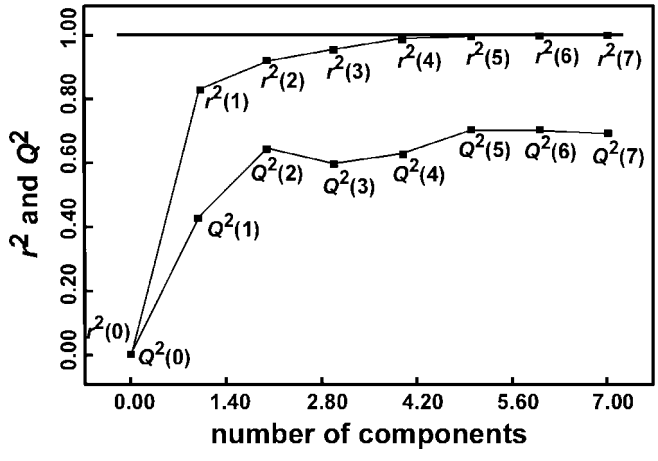

Figure 5. Comparison between fitted (r^2) and validated PLS model values, Q^2.

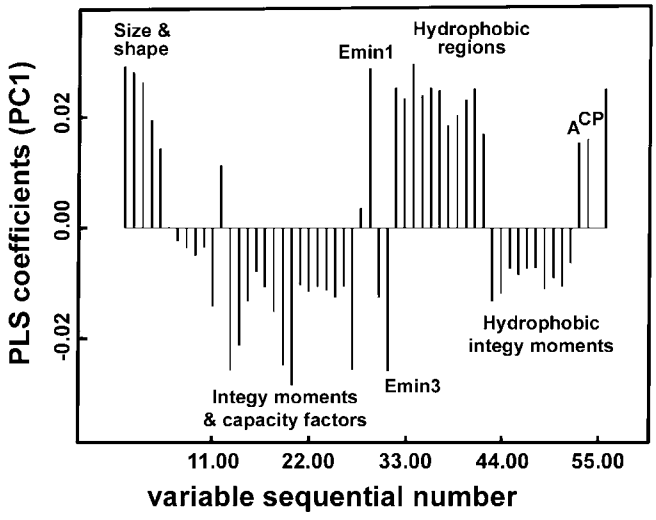

Figure 6. PLS coefficients plot for the global model for the correlation of VolSurf descriptors with log k_w^{RPLC} partitioning.

molecular globularity; all of them disclosed by the H_2O interaction probe. They are also positively correlated with hydrophobic regions as defined by DRY probe. The same trend is found for the amphiphilic moment and the critical packing parameter. (A) is a vector pointing from the center of the hydrophobic domain to the center of the hydrophilic one, and stresses the needed capability of compounds to penetrate the packed columns. These results are clearly in agreement with the GRID contour maps found for these molecules, as can be seen in Figure 7. Figure 7(a) shows the water map around molecule with a high concentration of hydrated region in only one small part of the molecules, namely those having the nitrogen heteroatoms in the mesoionic ring along with the exo-nitrogen. The high importance of this

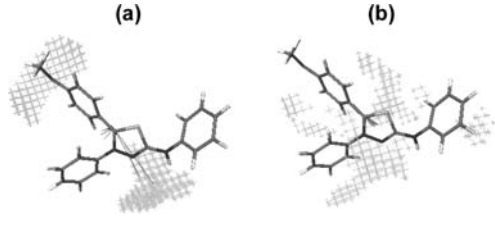

Figure 7. GRID maps for (a) water and (b) DRY probes countered at -3.23 and $-1.23\,\text{kcal mol}^{-1}$, respectively for compound 7. The hydrophilic fields are located nearby nitrogen and methoxy moieties, whereas the lipophilic ones hold close phenyl and mesoionic rings. The interaction energies (arrows) point to the centre of the regions.

region comes from the negatively correlated log k_w^{RPLC} with integy moments and retention factors. From the integy moments one may figure out that the polar nitrogen moieties are far away from the center of mesoionic masses, whereas the retention factors represent the balance between the amount of hydrophilic region and the surface unit, again highly concentrated into the hydrophilic region of such mesoionic compounds. The high magnitude values of integy moments indicate a clear concentration of hydrated region in one part of the molecule. The much smaller negative hydrophobic integy moments do favor this: they are similar to the integy moments, but rather calculated from DRY probe 3D interaction maps. They measure the unbalance between the center of mass of mesoionic molecules and the position of the hydrophobic regions around them (Figure 7(b)). There is also a negative hydrophilic-lipophilic interaction along with them, which are roughly equal balanced. They are located at the same region of the hydrophobic integy moments. The critical packing, CP, describes a ratio between the hydrophobic and hydrophilic part of the molecule, but in terms of shape, thus, in accordance with size and shape descriptors previously discussed. The hydrophilic regions are not important (small negative bars on the left), and are negatively correlated to log k_w^{RPLC} values. Taken as a whole, the presence of high integy moments and capacity factors are detrimental for partitioning, whereas the increase of hydrophobic regions (as demonstrated by the CP and D descriptors) favors partitioning, along with size and shape descriptors.

It is noteworthy how VolSurf descriptors have matched the π lipophilic constants for compounds 4 and 8. Close descriptors plot examination (Figure 8) of the two molecules unveils it. Compound 4 has a negative value for D1DRY profile (peak height of -1.25), whereas 8 has a positive D5DRY loading profile (peak of 1.53). These are defined when a DRY

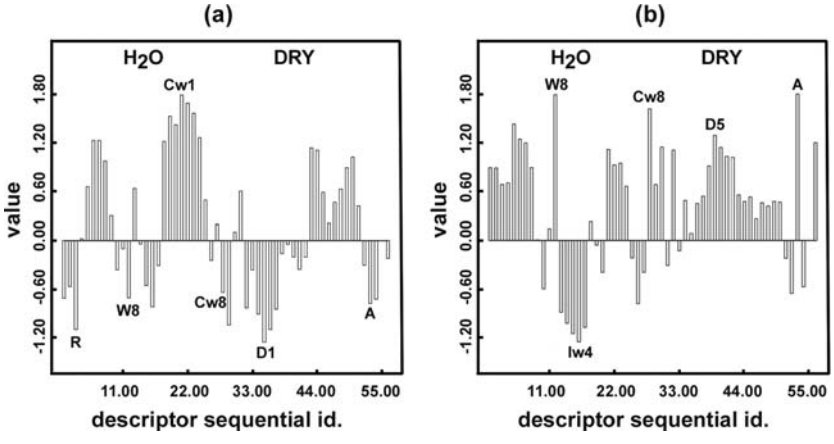

Figure 8. PLS descriptor loading plots of PC1 *versus* PC2 for compounds (a) 4 and (b) 8 of the model of Figure 3.

probe is interacting with the two molecules. The two hydrophobic regions indicate interactions with the hydrophobic probe at two different energy levels, which have been adapted to the energy range of the DRY probe (-0.2 and $-1.0\,\text{kcal mol}^{-1}$, respectively).

The amount of hydrophilic regions per surface unit, represented by the ratio between the hydrophilic regions and the total molecular surface, named capacity factor (Cw), is at the value of -0.54 in height for compound 4, and 1.91 for compound 8. Both values were calculated at $-8.0\,\text{kcal mol}^{-1}$ interaction energy level with the water probe. The high peak intensity found so far for compound 8 conceives it to bear a lipophilic moiety of nitro group. The high intense peak (2.43) of the amphiphilic moment (A) also confirms this, as discussed above. Accordingly, compound 4 has a peak intensity of -0.78. Note that this negative value is detrimental for partitioning from mobile to stationary phase. Again, this is in accordance with the chromatographic partition coefficient for this compound.

Another striking difference between these two compounds arises from hydrophilic regions themselves. Compound 8, has a high peak intensity value of 2.12, at the interaction energy level of -6 kcal mol^{-1}. For instance it accounts for polar and hydrogen bond donor-acceptor regions, as depicted in Figure 7. On the other hand, compound 4 has a small negative value for this descriptor. Consequently, the π_{nitro} contribution to overall log P value of compound 4 is of hydrophilic nature, and its contribution on log P for compound 8 is lipophilic.

Prediction of Log P from Isocratic Log k Values

Log P values can also be estimated from the retention factors, log k, instead of log k_w.[14] Albeit log k_w better accounts for lipophilicity differences among analytes, it is worthwhile seeing how log k_w is built thereupon the isocratic log k values. In order to derive the chromatographic retention factors to obtain log k_w, we have measured retention factors at MeOH:buffer 35, 45, 55, 65, and 75 v/v. Table 4 shows their values.

To begin with, it can be noticed from Table 4, that compounds become more "hydrophilic" with the increase of MeOH modifier content in the mobile phase. This means, analytes tend to stay in the mobile phase and not partitioning. Log k magnitude values at MeOH:buffer 65 and 75 v/v cannot correlate well with log P, and this is exactly what we have found from 3D MIF used so far in this work. The PLS goodness of fit and prediction begin only at MeOH:buffer 55 v/v, being of ca.: $r^2 = 0.871$, and $Q^2 = 0.501$. This is in agreement with Yamagami postulation.[14] However, our results demonstrate that diminishing the MeOH content in the mobile phase, and thus getting closer to log k_w, log k bears resemblance to log P_{app} magnitude values, as can thoroughly be seen in this paper. As a result, like Braumann,[62] we would like to recall that log k_w is not identical, but certainly it is quite similar to log P.

Table 4. Comparison between log P and log k values for PMOS column

Compound	log k_{35}[a]	log k_{45}	log k_{55}	log k_{65}	log k_{75}	$-S.10^{-2b}$
1	0.66	0.21	−0.04	−0.38	−0.55	3.3
2	1.01	0.56	0.24	−0.15	−0.43	3.7
3	0.90	0.42	0.08	−0.12	−0.48	3.4
4	0.68	0.28	0.08	−0.13	−0.51	3.0
5	1.20	0.72	0.37	−0.16	−0.62	4.5
6	1.48	1.11	0.58	−0.04	−0.46	4.9
7	1.33	0.78	0.48	−0.02	−0.51	4.5
8	1.28	0.78	0.49	−0.06	−0.54	4.5

[a]Log k values for percentages of MeOH: buffer (v/v) in the mobile phase.
[b]Log $k = -S\varphi + \log k_w$. See text for explanation.

This result also reinforces that partitioning is dependent of the composition of the mobile phase.

It has also been suggested that the slope obtained for log k versus MeOH content, φ_{MeOH}, S, is a measure of solvent strength.[63–65] The straight lines in the composite diagram found in Figure 9 are nearly parallel. However, as the methanol content approaches zero percent, the lines open up a bit. We reasoned the overestimating of log P values by log k_w, based on the role played by S. This descriptor encodes the molecular size, structure of the analytes and their capabilities of being H-donor, amphiphilic, or H-acceptor.[30] Equations (7)–(10), show the S dependence over log k_w and different log k. There is a linear relationship among them, but the slope is near one for log k_w (Equation (7). On the other hand, slopes among log k relationships are similar, but much higher then the one found in Equation (7) where there is a difference in the strength of H-bond domain when modifying the MeOH content in the mobile phase. That is, as the water enrichment takes place the capability of making H-bond gets stronger

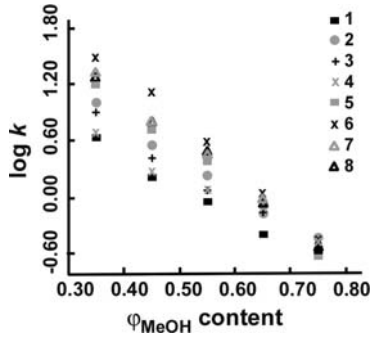

Figure 9. Composite relationships for all study mesoionic compounds between log k and the percentage of MeOH content.

(Equations (8)–(10)), and log k_w is overestimated. Accordingly, at high values of MeOH content there should be no strong differences in the H-bonding pattern for these mesoionic compounds. As we have already anticipated via Equations (5) and (6), the same trend is found when chromatographic retention coefficients are taken from ODS columns.

$$-S = 1.24\ (\pm 0.16)\ \log\ k_w + 0.91\ (\pm 0.41)$$
$$(\mathrm{n} = 8, r^2 = 0.982, s = 0.100, \mathrm{F} = 345.7, Q^2 = 0.967) \quad (7)$$

$$-S = 2.93\ (\pm 0.94)\ \log\ k_{\varphi 55} + 3.13\ (\pm 0.34)$$
$$(n = 8, r^2 = 0.906, s = 0.234, \mathrm{F} = 57.8, Q^2 = 0.818) \quad (8)$$

$$-S = 2.25\ (\pm 0.69)\ \log\ k_{\varphi 45} + 2.60\ (\pm 0.46)$$
$$(n = 8, r^2 = 0.914, s = 0.224, \mathrm{F} = 63.4, Q^2 = 0.816) \quad (9)$$

$$-S = 2.26\ (\pm 0.53)\ \log\ k_{\varphi 35} + 1.56\ (\pm 0.59)$$
$$(n = 8, r^2 = 0.947, s = 0.175, \mathrm{F} = 107.9, Q^2 = 0.902) \quad (10)$$

Extending the study further, and thus validating our finds, Van de Waterbeemd[63] pointed out that for a set of 233 compounds taken from different column types and lengths resulted in Equation (11) when S is plotted against log k_w. We have submitted the S values to our calculated MIF, and results show a clear correlation between them. The statistic parameters of goodness of fit and prediction are $r^2 = 0.946$, $Q^2 = 0.737$. The PLS loading plot (partial weights) of PC1 versus PC2 (not shown) is very similar to the one shown in Figure 4.

$$S = 1.04\ (\pm 0.06)\ \log\ k_w + 0.99\ (\pm 0.01)$$
$$(\mathrm{n} = 233, r^2 = 0, 968, s = 0.580, \mathrm{F} = 6974) \quad (11)$$

CONCLUSIONS

The robust results of the PLS model clearly demonstrate that it is possible to describe and predict RPLC partitioning from the 3D molecular structure of mesoionic 1,3,4-thyadiazolium-3-aminides. These models are in good agreement with known molecular features related to partitioning. VolSurf descriptors generated from water and DRY probes allowed the relevant 3D molecular properties to be disclosed. This might be valuable in optimizing the transport profile in terms of its 3D molecular interactions early in the drug design process.

Overall, using calculated molecular descriptors from 3D molecular interaction fields, the chromatographic partition coefficients were described. The GRID MIF encoded by VolSurf descriptors properly revealed the balanced interaction energies needed to impart and promote partitioning of the betaine-like molecules. The additivity scheme of calculated log *P* was also fulfilled. The 3D TSAR log *P* atom based calculations agreed with chromatographic measurements and was in conformity with the 3D molecular fields. The classical QSPR equations shown herein are also further validated by the 3D MIF. The extrathermodynamic relationships between partitioning of the same set of compounds against the two chromatographic stationary phases are in concurrence with the calculated MIF because the same descriptors were needed to characterize the chromatographic partitioning in both columns. The volume related terms, hydrophobic and electrostatic interactions were shown to be good and detrimental for partitioning, respectively; mostly emphasizing the balance between hydrophobic and hydrophilic interactions needed for describing chromatographic retention mechanism. The heteroatom contribution to partitioning is of key importance when ascribing H-bonding pattern for all mesoionics studies.

ACKNOWLEDGMENTS

The authors are indebted to the Brazilian Grating Agencies, FAPESP, CNPq, FAPEMIG, and FINEP.

REFERENCES

1. Eros, D.; Kovesdi, I.; Orfi, L.; Takacs-Novak, K.; Acsady, G.; Kevi, G. Reliability of log *P* predictions based on calculated molecular descriptors: A critical review. Curr. Med. Chem. **2002**, *9*, 1819–1829.
2. Bleicher, K.H.; Böhm, H.-J.; Müller, K.; Alanine, A.I. Hit and lead generation: Beyond high-throughput screening. Nat. Rev. Drug Discov. **2003**, *2*, 369–378.
3. (a) Livingstone, D.J. Theoretical property predictions. Curr. Top. Med. Chem. **2003**, *3*, 1171–1192; (b) Tetko, I.V.; Tanchuk, V.Y.; Kasheva, T.N.; Villa, A.E.P. Internet software for the calculation of the lipophilicity and aqueous solubility of chemical compounds. J. Chem. Inf. Comp. Sci. **2001**, *41*, 246–252.
4. Rees, D.C.; Congreve, M.; Murray, C.W.; Carr, R. Fragment-based lead discovery. Nat. Rev. Drug Discov. **2004**, *3*, 660–672.
5. Marrero, J.; Gani, R. Group-contribution-based estimation of octanol/water partition coefficient and aqueous solubility. Ind. Eng. Chem. Res. **2002**, *41*, 6623–6633.
6. (a) Hansch, C.; Leo, A. *Exploring QSAR. Fundamentals and Applications in Chemistry and Biology*. ACS Professional Reference Book; ACS: Washington, D.C., 1995, 557; (b) Hansch, C.; Leo, A.; Hoekman, D. *Exploring QSAR. Hydrophobic, Electronic, and Steric Constants*. ACS Professional Reference Book; ACS: Washington, D.C., 1995, 348.

7. (a) Mannhold, R.; Petrauskas, A. Substructure versus whole-molecule approaches for calculating log P. QSAR Comb. Sci. **2003**, *22*, 466–475; (b) Sun, H.M. A universal molecular descriptor system for prediction of LogP, LogS, LogBB, and absorption. J. Chem. Inf. Comput. Sci. **2004**, *44*, 748–757.
8. Mannhold, R.; van de Waterbeemd, H. Substructure and whole molecule approaches for calculating log P. J. Comput.-Aided Mol. Des. **2001**, *15*, 337–354.
9. (a) Abraham, M.H.; Ibrahim, A.; Zissimos, A.M.; Zhao, Y.H.; Comer, J.; Reynolds, D.P. Application of hydrogen bonding calculations in property based drug design. Drug Discov. Today **2002**, *7*, 1056–1063; (b) Abraham, M.H.; Zhao, Y.H. Determination of solvation descriptors for ionic species: Hydrogen bond acidity and basicity. J. Org. Chem. **2004**, *69*, 4677–4685.
10. Zou, J.W.; Zhao, W.N.; Shang, Z.C.; Huaang, M.L.; Guo, M.; Yu, Q.S. A quantitative structure-property relationship analysis of logP for disubstituted benzenes. J. Phys. Chem. A **2002**, *106*, 11550–11557.
11. (a) Buchwald, P. Modeling liquid properties, solvation, and hydrophobicity: A molecular size-based perspective. Perspect. Drug Discov. Des. **2000**, *19*, 19–45; (b) Klopman, G.; Zhu, H. Recent methodologies for the estimation of N-octanol/water partition coefficients and their use in the prediction of membrane transport properties of drugs. Mini-Rev. Med. Chem. **2005**, *5*, 127–133.
12. Valko, K.; Du, C.M.; Bevan, C.; Reynolds, D.P.; Abraham, M.H. Rapid method for the estimation of octanol/water partition coefficient (log P-oct) from gradient RP-HPLC retention and a hydrogen bond acidity term (Sigma alpha(H)(2)). Curr. Med. Chem. **2001**, *8*, 1137–1146.
13. Leo, A.J.; Hansch, C. Role of hydrophobic effects in mechanistic QSAR. Perspect. Drug Discov. Des. **1999**, *17*, 1–25.
14. Yamagami, C. Recent advances in reverse-phase-HPLC techniques to determine lipophilicity. In *Pharmacokinetic Optimization in Drug Research. Biological, Physicochemical, and Computational Strategies*; Testa, B., van de Waterbeemd, H., Folkers, G., Guy, R., Eds.; Wiley-VCH: Weinheim, Germany, 2001; 383–400.
15. Yamagami, C.; Kawase, K.; Iwaki, K. Hydrophobicity parameters determined by reversed-phase liquid chromatograph. XV: Optimal conditions for prediction of log P-oct by using RP-HPLC procedures. Chem. Pharm. Bull. **2002**, *50*, 1578–1583.
16. de Athayde, P.F.; Miller, J.; Simas, A.M. Mesoionic compounds: Amphiphilic heterocyclic betaines. Synthesis-Stuttgart **2000**, *11*, 1565–1568.
17. da Silva, E.F.; Canto-Cavalheiro, M.M.; Braz, V.R.; Cysne-Finkelstein, L.; Leon, L.L.; Echevarria, A. Synthesis, and biological evaluation of new 1,3,4-thiadiazolium-2-phenylamine derivatives against Leishmania amazonensis promastigotes and amastigotes. Eur. J. Med. Chem. **2002**, *37*, 979–984.
18. Schonafinger, K. Heterocyclic NO prodrugs. Farmaco **1999**, *54*, 316–320.
19. Gryglewski, R.J.; Marcinkiewicz, E.; Robak, J.; Michalska, Z.; Madej, J. Mesoionic oxatriazoles (MOTA): NO-donating characteristics and pharmacology. Curr. Pharm. Design **2002**, *8*, 167–176.
20. Cadena, S.M.S.C.; Carnieri, E.G.S.; Echevarria, A.; de Oliveira, M.B.M. Effect of MI-D, a new mesoionic compound, on energy-linked functions of rat liver mitochondria. Febs Lett. **1998**, *440*, 46–50.
21. Hellberg, M.; Stubbins, J.F.; Glennon, R.A. A preliminary investigation of mesoionic xanthine analogues as inhibitors of platelet aggregation. Bioorg. Med. Chem. **2000**, *8*, 1917–1923.

22. Montanari, C.A. Medicinal chemistry – contribution and outlook in the development of pharmacotherapy. Quim. Nova **1995**, *18*, 56–64.
23. Montanari, C.A.; do Amaral, A.T.; Giesbrecht, A.M. Synthesis and antibacterial activity of some new 1,3,4-thiadiazolium-2-aminide derivatives. Pharm. Sci. **1997**, *3*, 565–568.
24. (a) Senff-Ribeiro, A.; Echevarria, A.; Silva, E.F.; Franco, C.R.; Veiga, S.S.; Oliveira, M.B. Cytotoxic effect of a new 1,3,4-thiadiazolium mesoionic compound (MI-D) on cell lines of human melanoma. Br. J. Cancer **2004**, *19*, 297–304; (b) Senff-Ribeiro, A.; Echevarria, A.; Silva, E.F.; Veiga, S.S.; Oliveira, M.B. Antimelanoma activity of 1,3,4-thiadiazolium mesoionics: a structure-activity relationship study. Anticancer Drugs **2004**, *15*, 269–275.
25. Montanari, CA.; Sandall, J.P.B.; Miyata, Y.; Miller, J. Structural studies on some 1,3,4-thiadiazolium-2-aminides and their rearrangement isomers using N-15 and C-13 NMR-spectroscopy. J. Chem. Soc. Perk. Trans. **1994**, *2*, 2571–2575 (Erratum: J. Chem. Soc. Perkin. Trans. **1995** 2 2375).
26. dos Santos, A.C.S.; Echevarria, A. Electronic effects on C-13 NMR chemical shifts of substituted 1,3,4-thiadiazolium salts. Magn. Reson. Chem. **2001**, *39*, 182–186.
27. (a) Simas, A.M.; Miller, J.; de Athayde, P.F. Are mesoionic compounds aromatic? Can. J. Chem. **1998**, *76*, 869–872; (b) Balaban, A.T.; Oniciu, D.C.; Katritzky, A.R. Aromaticity as a cornerstone of heterocyclic chemistry. Chem. Rev. **2004**, *104*, 2777–2812.
28. Echevarria, A.; Galembeck, S.E.; Maciel, M.A.M.; Miller, J.; Montanari, C.A.; Rumjanek, V.M.; Simas, A.M.; Sandall, J.P.B. Reaction of aroyl chlorides with 1,4-diphenylthiosemicarbazide: formation of both 1,3,4-thiadiazolium-2-aminides and 1,3,4-triazolium-2-thiolate. Heterocycl. Commun. **1995**, *1*, 129–136.
29. Cheung, K.K.; Echevarria, A.; Galembeck, S.; Maciel, M.A.M.; Miller, J.; Rumjanek, V.M.; Simas, A.M. Mesoionic compounds. 4. Structure of 1,4,5-triphenyl-1,2,4-triazolium-3-thiolate. Acta Crystal. **1993**, *C 49*, 1092–1094.
30. Britto, M.M.; Montanari, C.A.; Donnici, C.L.; Cass, Q.B. On the partitioning of some newly synthesized mesoionic 1,3,4-thiadiazolium-2-aminide and precursors evaluated by RP-HPLC. J. Liq. Chromatogr. & Rel. Technol. **1999**, *22*, 357–366.
31. Perisic-Janjic, N.U.; Acanski, M.M.; Janjic, N.J.; Lazarevic, M.D.; Dimova, V. Study of the lipophilicity of some 1,2,4-triazole derivatives by RPHPLC and TLC. J. Planar. Chromatogr. **2000**, *13*, 281–284.
32. Mazza, C.B.; Whitehead, C.E.; Breneman, C.M.; Cramer, S.M. Predictive quantitative structure retention relationship models for ion-exchange chromatography. Chromatographia **2002**, *56*, 147–152.
33. Luke, B.T. Comparison of three different QSAR/QSPR generation techniques. J. Mol. Struct.-Theochem. **1999**, *468*, 13–20.
34. von Roedern, E.G. A new method for the characterization of chemical libraries—solely by HPLC retention times. Mol. Divers. **1998**, *3*, 253–256.
35. Nasal, A.; Siluk, D.; Kaliszan, R. Chromatographic retention parameters in medicinal chemistry and molecular pharmacology. Curr. Med. Chem. **2003**, *10*, 381–426.
36. Espinosa, S.; Bosch, E.; Roses, M.; Valko, K. Change of mobile phase pH during gradient reversed-phase chromatography with 2,2,2-trifluoroethanol-water as mobile phase and its effect on the chromatographic hydrophobicity index determination. J. Chromatogr. A **2002**, *954*, 77–87.

37. Camurri, G.; Zaramella, A. High-throughput liquid chromatography/mass spectrometry method for the determination of the chromatographic hydrophobicity index. Anal. Chem. **2001**, *73*, 3716–3722.
38. Dorsey, J.G.; Cooper, W.T.; Siles, B.A.; Foley, J.P.; Barth, H.G. Liquid chromatography: Theory and methodology. Anal. Chem. **1998**, *70*, 591R–644R.
39. Du, C.M.; Valko, K.; Bevan, C.; Reynolds, D.; Abraham, M.H. Rapid gradient RP HPLC method for lipophilicity determination: A solvation equation based comparison with isocratic methods. Anal. Chem. **1998**, *70*, 4228–4234.
40. Lazaridis, T. Solvent size vs cohesive energy as the origin of hydrophobicity. Accounts Chem. Res. **2001**, *34*, 931–937.
41. Matulis, D.; Bloomfield, V.A. Thermodynamics of the hydrophobic effect. II. Calorimetric measurement of enthalpy, entropy, and heat capacity of aggregation of alkylamines and long aliphatic chains. Biophys. Chem. **2001**, *93*, 53–65.
42. Kim, K.H. Thermodynamic aspects of hydrophobicity and biological QSAR. J. Comput.-Aided Mol. Des. **2001**, *15*, 367–380.
43. Gallicchio, E.; Kubo, M.M.; Levy, R.M. Enthalpy-entropy and cavity decomposition of alkane hydration free energies: Numerical results and implications for theories of hydrophobic solvation. J. Phys. Chem. B **2000**, *104*, 6271–6285.
44. Britto, M.M.; Montanari, C.A.; Donnici, C.L.; Cass, Q.B. On the synthesis of mesoionic 1,3,4-thiadiazolium-2-aminide and precursors. Heterocycl. Commun. **1998**, *4*, 209–216.
45. Anazawa, T.A.; Jardim, I.C.S.F. The chromatographic behavior of coated stationary phases with different silicas. J. Liq. Chromatogr. & Rel. Technol. **1998**, *21*, 645–655.
46. Sybyl Version 6.5.3, Tripos, Inc., Saint Louis, U.S.A. 1999.
47. 3D TSAR, Version 3.2.1, Oxford Molecular, Ltd., Oxford, U.K. 1998.
48. Cruciani, G.; Pastor, M.; Guba, W. VolSurf: a new tool for the pharmacokinetic optimization of lead compounds. Eur. J. Pharm. Sci. **2000**, *11* (2), S29–S39.
49. Cruciani, C.; Crivori, P.; Carrupt, P.A.; Testa, B. Molecular fields in quantitative structure-permeation relationships: the VolSurf approach. J. Mol. Struct.-Theochem **2000**, *503*, 17–30.
50. Cruciani, G.; Pastor, M.; Mannhold, R. Suitability of molecular descriptors for database mining. A comparative analysis. J. Med. Chem. **2002**, *45*, 2685–2694.
51. Cruciani, G.; Pastor, M.; Guba, W. VolSurf: a new tool for the pharmacokinetic optimization of lead compounds. Eur. J. Pharm. Sci. **2000**, *11*, S29–S39.
52. GRID version 20 Molecular Discovery Ltd., London, U.K., 2002.
53. Goodford, P.J. A computational procedure for determining energetically favorable binding-sites on biologically important macromolecules. J. Med. Chem. **1985**, *28*, 849–857.
54. Boobbyer, D.N.A.; Goodford, P.J.; McWhinnie, P.M.; Wade, R.C. New hydrogen-bond potentials for use in determining energetically favorable binding-sites on molecules of known structure. J. Med. Chem. **1989**, *32*, 1083–1094.
55. Wade, R.C.; Clark, K.J.; Goodford, P.J. Further development of hydrogen-bond functions for use in determining energetically favorable binding-sites on molecules of known structure.1. Ligand probe groups with the ability to form 2 hydrogen-bonds. J. Med. Chem. **1993**, *36*, 140–147.
56. Cruciani, G.; Clementi, S.; Crivori, P.; Carrupt, P.-A.; Testa, B. VolSurf and its application in structure-disposition relationships. In *Pharmacokinetic Optimization in Drug Research: Biological, Physicochemical, and Computational Strategies*; Testa, B., van de Waterbeemd, H., Folkers, G., Guy, R., Eds.; Wiley-VCH: Weinheim, Germany, 2001; 539–550.

57. Oprea, T.I.; Zamora, I.; Ungell, A.-L. Pharmacokinetically based mapping device for chemical space navigation. J. Comb. Chem. **2002**, *4*, 258–266.
58. Montanari, C.A.; Cass, Q.B.; Tiritan, M.E.; Souza, A.L.S. A QSERR study on enantioselective separation of enantiomeric sulphoxides. Anal. Chim. Acta **2000**, *419*, 93–100.
59. Montanari, M.L.C.; Cass, Q.B.; Montanari, C.A. Quantitative structure-retention relationships of antimicrobial hydrazides evaluated by reverse-phase liquid chromatography. Chromatographia **2000**, *51*, 722–726.
60. Montanari, M.L.C.; Montanari, C.A.; Pilo-Veloso, D.; Cass, Q.B. Estimation of the RP-HPLC lipophilicity parameters log k′, and log k(w), a comparison with the hydrophobicity index phi(0). J. Liq. Chromatogr. & Rel. Technol. **1997**, *20*, 1703–1715.
61. Ooms, F.; Weber, P.; Carrupt, P.A.; Testa, B. A simple model to predict blood-brain barrier permeation from 3D molecular fields. BBA-Mol. Basis Dis. **2002**, *1587*, 118–125.
62. Braumann, T. Determination of hydrophobic parameters by reversed-phase liquid-chromatography: theory, experimental-techniques, and application in studies on quantitative structure-activity relationships. J. Chromatogr. **1986**, *373*, 191–225.
63. Van de Wateerbemd, H.; Kansy, M.; Wagner, B.; Fischer, H. Lipophilicity in drug action and toxicology. In *Methods and Principles in Medicinal Chemistry*; Mannhold, R., Kubinyi, H., Timmerman, H., Eds.; Wiley-VCH: Weinheim, Germany, 1996; Vol. 4, 73–87.
64. Kansy, M.; Fischer, H.; Van de Waterbeemd, H. In *QSAR and Molecular Modelling: Concepts, Computational Tools and Biological Applications*. Proceedings of the 10th European Symposium on Structure-Activity Relationships: QSAR and Molecular Modelling; Barcelona, Spain, Sept 4–9, 1994; Sanz, F., Giraldo, J., Manaut, F., Eds.; J.R. Prous, S. A.: Barcelona, 1995.
65. Minick, D.J.; Brent, D.A.; Frenz, J. Modeling octanol water partition-coefficients by reversed-phase liquid-chromatography. J. Chromatogr. **1989**, *461*, 177–191.

Received August 11, 2005
Accepted September 20, 2005
Manuscript 6697